Earth and Planetary Science Letters 477 (2017) 97–107

Contents lists available at ScienceDirect

Earth and Planetary Science Letters

www.elsevier.com/locate/epsl

Cretaceous–Eocene provenance connections between the Palawan Continental Terrane and the northern South China Sea margin

Lei Shao [a], Licheng Cao [a,*], Peijun Qiao [a], Xiangtao Zhang [b], Qianyu Li [a], Douwe J.J. van Hinsbergen [c]

[a] State Key Laboratory of Marine Geology, Tongji University, Shanghai 200092, China
[b] Shenzhen Branch of China National Offshore Oil Corporation, Guangzhou 510240, China
[c] Department of Earth Sciences, Utrecht University, Heidelberglaan 2, 3584 CS Utrecht, Netherlands

ARTICLE INFO

Article history:
Received 17 April 2017
Received in revised form 11 August 2017
Accepted 14 August 2017
Available online 1 September 2017
Editor: A. Yin

Keywords:
South China Sea
Palawan
provenance
U–Pb geochronology
heavy mineral

ABSTRACT

The plate kinematic history of the South China Sea opening is key to reconstructing how the Mesozoic configuration of Panthalassa and Tethyan subduction systems evolved into today's complex Southeast Asian tectonic collage. The South China Sea is currently flanked by the Palawan Continental Terrane in the south and South China in the north and the two blocks have long been assumed to be conjugate margins. However, the paleogeographic history of the Palawan Continental Terrane remains an issue of uncertainty and controversy, especially regarding the questions of where and when it was separated from South China. Here we employ detrital zircon U–Pb geochronology and heavy mineral analysis on Cretaceous and Eocene strata from the northern South China Sea and Palawan to constrain the Late Mesozoic–Early Cenozoic provenance and paleogeographic evolution of the region testing possible connection between the Palawan Continental Terrane and the northern South China Sea margin. In addition to a revision of the regional stratigraphic framework using the youngest zircon U–Pb ages, these analyses show that while the Upper Cretaceous strata from the Palawan Continental Terrane are characterized by a dominance of zircon with crystallization ages clustering around the Cretaceous, the Eocene strata feature a large range of zircon ages and a new mineral group of rutile, anatase, and monazite. On the one hand, this change of sediment compositions seems to exclude the possibility of a latest Cretaceous drift of the Palawan Continental Terrane in response to the Proto-South China Sea opening as previously inferred. On the other hand, the zircon age signatures of the Cretaceous–Eocene strata from the Palawan Continental Terrane are largely comparable to those of contemporary samples from the northeastern South China Sea region, suggesting a possible conjugate relationship between the Palawan Continental Terrane and the eastern Pearl River Mouth Basin. Thus, the Palawan Continental Terrane is interpreted to have been attached to the South China margin from the Cretaceous until the Oligocene oceanization of the South China Sea. In our preferred paleogeographic scenario, the sediment provenance in the northeastern South China Sea region changed from dominantly nearby Cretaceous continental arcs of the South China margin to more distal southeastern South China in the Eocene.

1. Introduction

The eastern margin of Eurasia was above the long-lived Panthalassa subduction zone consuming the Izanagi and Pacific plates during the Mesozoic (Müller et al., 2016). Since the Late Cretaceous this convergent setting along the South China margin has become diachronously and episodically replaced by continental rifting (Franke et al., 2014; Morley, 2016). Subsequent oceanic opening of the South China Sea (SCS; Fig. 1) in the Oligocene–Early Miocene has been traditionally viewed as a consequence of either the strain transfer from southeastward extruding Indochina along the Red River Fault (Fig. 2a; Briais et al., 1993; Leloup et al., 2001) or slab pull derived from subducting a hypothetical Proto-SCS beneath Borneo (Fig. 2b; Taylor and Hayes, 1983; Hall, 2002). Palawan, an island of the Philippines to the south of the SCS, exposes Upper Paleozoic to Mesozoic metamorphic and sedimentary rocks (Fig. 1a) that clearly show an Asian mainland origin based on paleomagnetism and provenance analysis (e.g., Almasco et al., 2000; Suzuki et al., 2000; Suggate et al., 2014). The continent-derived nature of these rocks is distinct from that of the

* Corresponding author at: State Key Laboratory of Marine Geology, Tongji University, 1239 Siping Road, Shanghai 200092, China.
E-mail address: licheng.cao@gmail.com (L. Cao).

http://dx.doi.org/10.1016/j.epsl.2017.08.019
0012-821X/

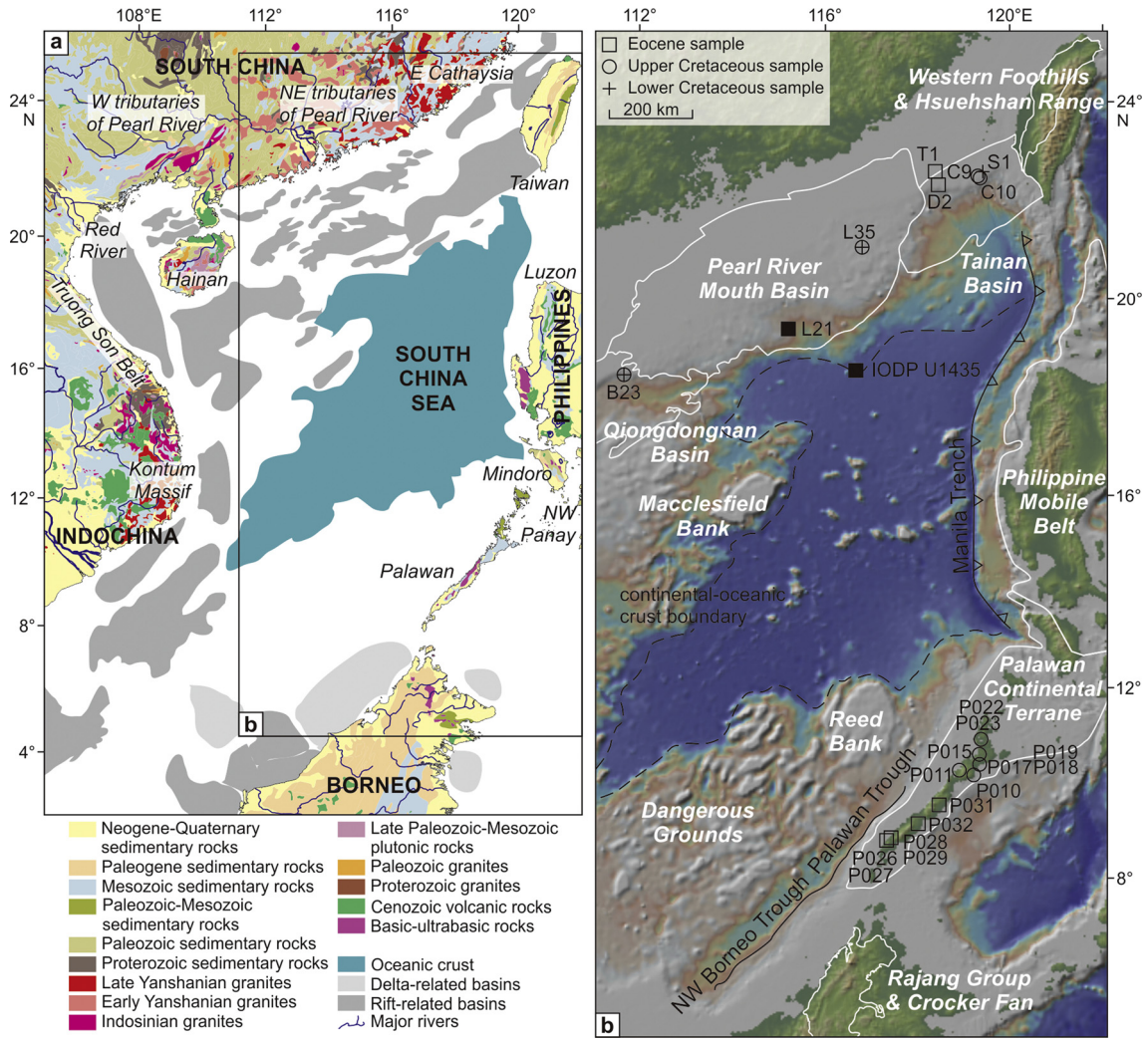

Fig. 1. (a) Geological map of Southeast Asia surrounding the SCS region. (b) Topographic map of the study area showing sample locations. Rift basins in the northern SCS margin, the PCT, the Philippine Mobile Belt, as well as the Eocene tectono-sedimentary units of West Taiwan and North Borneo are schematically outlined with white lines. The localities of commercial borehole L21 and IODP Site U1435 are also marked. (For interpretation of the references to color in this figure legend, the reader is referred to the web version of this article.)

Philippine Mobile Belt to the northeast which comprises a complex collage of island arcs and ophiolites (Fig. 1). Thus, Palawan as a component of the Palawan Continental Terrane (PCT) has long been supposed to start drifting along with the seafloor spreading processes in the SCS region (Holloway, 1982). However, the Late Mesozoic–Early Cenozoic paleogeographic history of the PCT remains controversial, especially with regard to its pre-drift location along the South China margin and the timing of drift initiation.

Ideally, the PCT's pre-drift location can be indirectly determined by reconstructing the SCS seafloor spreading history. This reconstruction process, however, is hampered by the SCS oceanic lithosphere that subducted eastward along the Manila Trench since the Miocene, and in addition, magnetic anomalies in the SCS are difficult to interpret due to strong post-spreading volcanism and ridge jumps (Fig. 1b; Taylor and Hayes, 1983; Briais et al., 1993; Sibuet et al., 2016). Attempts have been made towards a full-fit reconstruction by restoring the paleo-continental and oceanic crust boundary (e.g., Bai et al., 2015), but still involve significant uncertainties, particularly in defining the initial basement thickness and spatial distributions of conjugate margins. In these previous kinematic reconstructions, the proposed conjugate margins of the PCT include the Tainan Basin (e.g., Taylor and Hayes, 1983) and the Pearl River Mouth Basin (e.g., Sibuet et al., 2016), but these hypotheses have still not been verified by any independent evidence.

The controversy over the timing of drift initiation hinges on the interpretation of the tectonic nature of the Palawan Trough (Fig. 1b). In earlier tectonic reconstructions using either the extrusion model or the slab pull model, the PCT drifted southward in response to the Oligocene opening of the SCS (Figs. 2a and 2b; Holloway, 1982; Taylor and Hayes, 1983; Briais et al., 1993; Hall, 2002). The Palawan Trough has been accordingly assumed to be a bathymetric expression of extensional faults related to the Early Cenozoic rifting, and its contiguous juxtaposition with the Northwest Borneo Trough seems coincidental (Fig. 1b; Schlüter et al., 1996). Alternatively, the Northwest Borneo–Palawan Trough may represent an ancient trench marking a southeastward subduction of the Proto-SCS lithosphere beneath both Palawan and North Borneo (Hutchison, 2010; Cullen, 2014), which requires that the PCT was already located on the south side of the Proto-SCS during the Eocene (Fig. 2c). Thus, the PCT has been proposed to have been split off from the South China margin as early as the latest Cretaceous when the Proto-SCS formed presumably as a backarc basin to its northwest above the Izanagi subduction zone (Morley, 2012; Zahirovic et al., 2014). In this model, kinematic reconstruction of the Cenozoic PCT is inevitably sketchy because of the uncertainty associated with the now-vanished Proto-SCS crust.

Sediment provenance data can play a critical role in testing the paleogeographic and tectonic models described above. While pre-

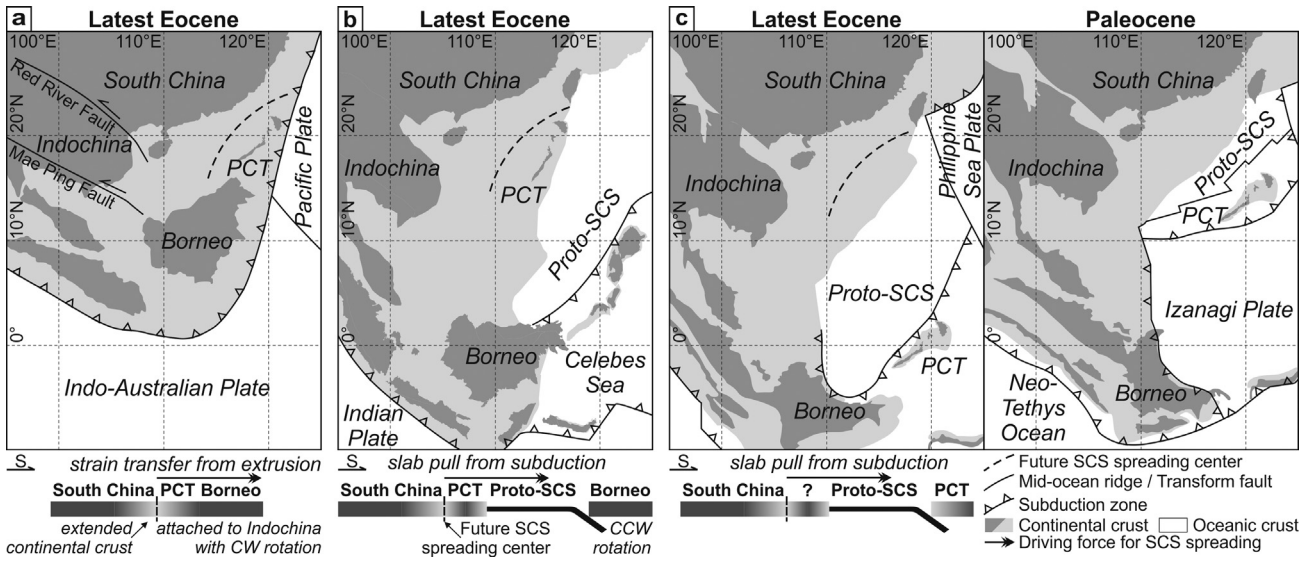

Fig. 2. Schematic models illustrating spreading mechanisms of the SCS and corresponding locations of the PCT during the latest Eocene. (a) The extrusion model (Briais et al., 1993; Leloup et al., 2001): the PCT and Borneo were attached to Indochina as a single rigid block that was extruded to the southeast with clockwise rotation due to the India–Eurasia collision. (b) The slab pull model (Taylor and Hayes, 1983; Hall, 2002): the subduction of a hypothetical Proto-SCS underneath North Borneo compensated the contemporaneous opening of the SCS. (c) A variant of the slab pull model with the PCT's location on the south side of the Proto-SCS, which assumes an earlier drift of the PCT in response to the Proto-SCS opening (Morley, 2012; Zahirovic et al., 2014).

vious provenance studies conducted in Palawan mainly focused on the Mesozoic strata (e.g., Walia et al., 2012; Suggate et al., 2014), it is unknown that whether the Lower Cenozoic strata were also sourced from South China. Also, a missing but essential link in this source-to-sink relationship is the Palawan's conjugate margin. The geological correlation between the PCT and its conjugate margin has been poorly understood due to limited borehole coverage of deep sediments in the northern SCS, and their poorly dated stratigraphy. In this paper, we investigate the detrital zircon U–Pb age and heavy mineral signatures of Cretaceous–Eocene strata from Palawan and several localities along the northern SCS margin. In strata lacking microfossils sufficient for high-resolution biostratigraphy, the youngest zircon U–Pb ages can provide valuable insight into the maximum depositional age (Dickinson and Gehrels, 2009), and thus facilitate stratigraphic correlations between sediments of both margins. The regional paleogeographic reconstruction obtained by integrating published provenance data with our new data allows us to address the following questions: 1) Where was the PCT approximately located along the South China margin at the timing of crustal breakup? and 2) Did seafloor spreading of the SCS since the Oligocene, or of a pre-Oligocene Proto-SCS caused the southward drift of the PCT? This study contributes to a better understanding of geodynamic history of the SCS region.

2. Regional geology and stratigraphy

2.1. Potential source areas

Before the final amalgamation of the Philippine Mobile Belt in today's East Philippines, the eastern border of the SCS region was likely a free boundary from Cretaceous to Eocene (Taylor and Hayes, 1983; Hall, 2002). With respect to regional lithological distribution and geographic location of the study area, potential source terranes in Indochina and South China are tentatively divided into seven zones from southwest to northeast (Fig. 1a). The well-confined zircon U–Pb age database derived from modern sediments and bedrocks in these two blocks is used to illustrate their provenance signatures (Fig. 3). Borneo in the south, however, is not considered as an important source area because it is a composite region of Gondwana-derived fragments that were not fully amalgamated in the promontory of Southeast Asia until the Late Mesozoic (Breitfeld et al., 2017). Nevertheless, published heavy mineral and detrital zircon age data from the Eocene deep marine turbidites of North Borneo (Rajang Group and Crocker Fan; Fig. 1b) are later compared with data obtained from the contemporary strata of Palawan so as to investigate whether or not these sediments were derived from similar provenances.

In eastern Indochina, the Truong Son Belt consists primarily of elongated zones of Paleozoic–Mesozoic sedimentary and metamorphic rocks, while the Kontum Massif is an uplifted block of high-grade metamorphic rocks intruded by granitic bodies and extensively covered by Neogene basalts (Fig. 1; Nagy et al., 2001). Magmatic and detrital zircons from these two zones are generally dated with Hercynian–Indosinian (200–300 Ma) ages peaking at ca. 250 Ma as well as a minor population of Meso–Neoproterozoic and Caledonian (400–500 Ma) ages (Fig. 3). The Red River is mainly fed by Mesozoic sedimentary rocks in the upstream region and widespread schists and gneisses along the downstream Red River Fault (Leloup et al., 2001). Detrital zircons from this drainage basin feature a multimodal U–Pb age distribution ranging from Paleoproterozoic to Cenozoic. Farther east, the age signatures of the Pearl River are grouped into two parts: a dominant population of Paleozoic–Mesozoic ages in its northeastern tributaries draining felsic igneous rocks; and a wide Paleoproterozoic to Mesozoic age range in its western tributaries draining carbonate and sedimentary rocks (Figs. 1 and 3). Major age peaks of the former group are also recognized in age data of river sediments from eastern Cathaysia. Hainan is dominated by intermediate-felsic intrusions, and their zircon U–Pb ages mostly cluster at Yanshanian (70–190 Ma) and Hercynian–Indosinian events.

Although the age signatures of aforementioned source terranes are diagnostic to some degree, it should be noted that they are only representative of modern topographic framework, as river courses have changed dramatically during the topographic reversal of East Asia from west-tilting to east-tilting (Wang, 2004). In addition to the today existing landmass, intrabasinal uplifts of various lithologies and ages which are now submerged beneath the northern SCS (Sun et al., 2014) could also have provenance potential.

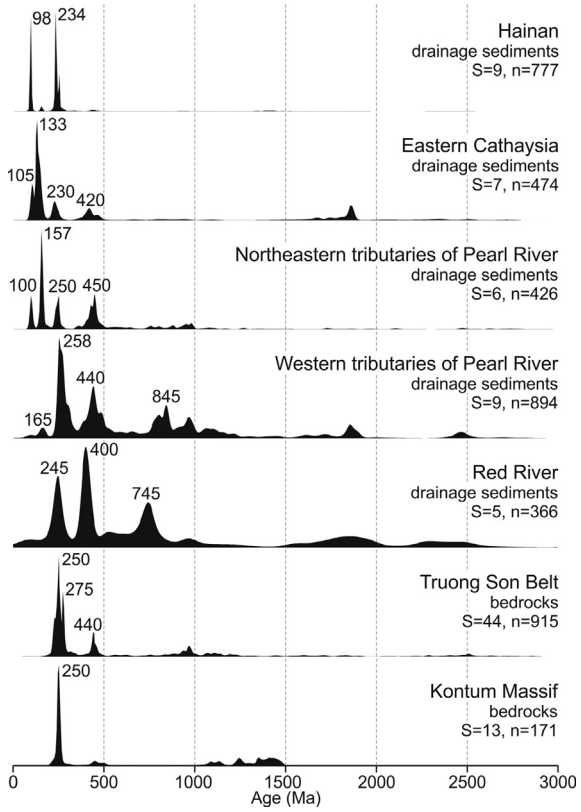

Fig. 3. Kernel density estimation (KDE) spectra of published zircon U–Pb ages from potential source terranes of the SCS region. Age data are preferentially acquired from detrital zircons in order to minimize biases resulting from sampling strategy and preservation potential, and the data selection follows the method described in the third section. S—number of samples, n—number of concordant analyses. See Supplementary Table S1 for compiled age data and references.

2.2. Northern SCS margin

The Early Cenozoic extension in the northern SCS margin appears to have propagated from northeast to southwest, with rift initiation first in the present-day West Taiwan region and the central part of the Pearl River Mouth Basin during the Late Paleocene, and later in the Qiongdongnan Basin and the southern part of the Pearl River Mouth Basin during the Middle Eocene (Fig. 1b; Lin et al., 2003; Morley, 2016). Extensive seismic data have revealed largely comparable basin architectures manifested by the formation of half-grabens and strongly asymmetric grabens, and the overlying wedge-shaped syn-rift infill (Franke et al., 2014). While the Paleocene sequence in the majority of the northern SCS is still poorly known (Morley, 2016), the Eocene strata are generally characterized by fluvial, lacustrine, and deltaic facies with occasional volcaniclastic intercalations (Lan et al., 2016; Shao et al., 2016, 2017). The recent inter-borehole comparison of planktonic foraminiferal and nannofossil records also found further expression of diachronous rifting in that marine deposition started earlier in the Paleocene in the Taiwan region before gradually expanding southwestward into the Pearl River Mouth Basin in the Middle Eocene (Li et al., 2016).

Until now, a limited number of commercial boreholes in the northern SCS have penetrated into the pre-Cenozoic strata and regional stratigraphic correlations have been tentatively made (Li et al., 2008; Sun et al., 2014). A marine regression sequence generally characterizes the Cretaceous deposition. The Lower Cretaceous strata drilled from the Tainan Basin and the eastern Pearl River Mouth Basin are mainly composed of shales, mudstones, siltstones, and sandstones of littoral and lacustrine facies. By contrast, the occurrence of gypsum cement in the Upper Cretaceous purplish sandstones of the Pearl River Mouth Basin represents an arid terrestrial sedimentary environment (Shao et al., 2007).

In addition to sedimentary rocks, widespread felsic-intermediate intrusive rocks and associated volcanics of Yanshanian ages have also been drilled on the northern SCS margin (e.g., Sun et al., 2014; Yan et al., 2014). These igneous rocks can be geochemically correlated with those widely distributed in South China and Indochina (Fig. 1a), which were generally formed in a continental arc setting during the Middle–Late Mesozoic, contrasting with the Early Cenozoic bimodal magmatism in coastal South China and the Late Cenozoic intraplate magmatism within the SCS oceanic basin (Yan et al., 2014). Notably, the Jurassic–Cretaceous magmatic rocks from the northern SCS margin and South China largely exhibit a pronounced northeast-striking distribution and a southeastward younging trend of ages (e.g., Zhou and Li, 2000; Li et al., 2014), which has been interpreted to be a consequence of rollback of the Izanagi slab (Li et al., 2012; Zahirovic et al., 2014).

2.3. Palawan

Palawan is generally subdivided into North and South Palawan on both sides of the NS-trending Ulugan Fault, based on the stratigraphic and structural contrasts of the two parts (Fig. 4). The oldest basement rocks exposed in North Palawan are represented by Permian to Jurassic olistostromes and oceanic plate stratigraphy, including the Bacuit Formation, the Liminangcong Formation, the Minilog Limestone, and the Guinlo Formation (Fig. 4; Aurelio and Peña, 2010). Overlying these non-metamorphic accretionary wedges is the Barton Group, a thick sequence composed of schists, phyllites, slates, sandstones, and shales, which can be further subdivided into the Caramay Schist, the Concepcion Phyllite, and the turbiditic Boayan Formation based on a decreasing degree of metamorphism. The depositional age of this continuous unit was recently constrained to the Late Cretaceous based on the presence of the coccolith *Prediscophaera cretacea* (Aurelio and Peña, 2010) and the youngest zircon crystallization ages (Walia et al., 2012).

The stratigraphic grouping of the PCT to which North Palawan belongs traditionally includes Southwest Mindoro, Romblon Island Group, and Northwest Panay, but not South Palawan because a dismembered ophiolitic terrane stretches from southern to central Palawan for about 300 km along the trend of the island (Figs. 1 and 4; Holloway, 1982; Encarnación et al., 1995). Two age intervals of the ophiolite crystallization were earlier determined by limited biostratigraphic and radiometric data: a structurally upper one of Eocene age and a lower one of Cretaceous age in tectonic windows beneath the Eocene ophiolites (Encarnación et al., 1995). However, according to the offshore seismic and onshore structural data (Schlüter et al., 1996; Aurelio et al., 2014), these ophiolites are actually emplaced over the Eocene turbidites (Panas Formation) along thrust structures best preserved in the ophiolite-turbidite contact as well as within the ophiolites, which are sealed by the overlying Lower–Middle Miocene shallow marine carbonates and clastics (Ransang Formation and Isugod Formation) (Fig. 4). Recent geochemical and high-precision geochronological investigations on the Eocene ophiolite and its underlying metamorphic sole pairs exposed along the Ulugan Fault also revealed that the oceanic crust in central Palawan was generated at the end of the Eocene (ca. 35 Ma) presumably at a mid-ocean ridge, shortly followed by subduction initiation and metamorphic sole formation less than 1 My later (Keenan et al., 2016). Thus, North and South Palawan seem to exist as a contiguous single unit within the PCT.

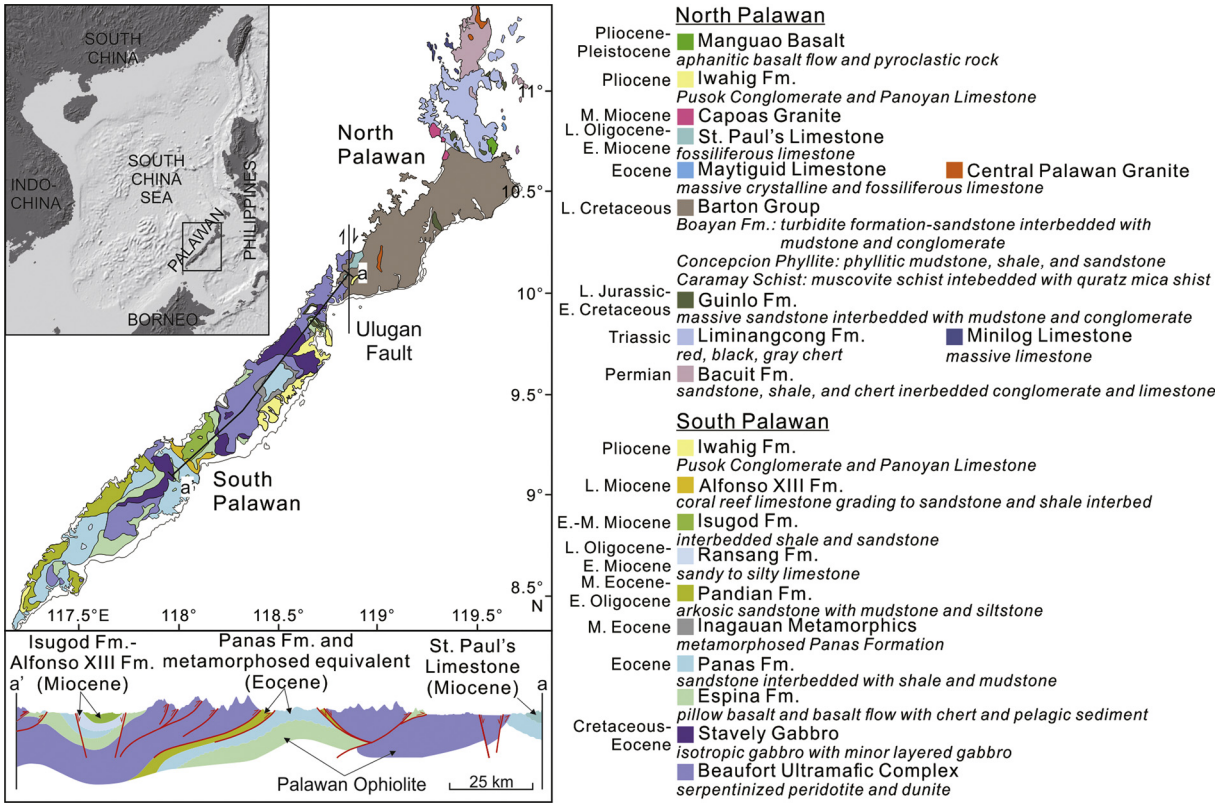

Fig. 4. Geological map of Palawan showing stratigraphic framework and lithological distribution (modified from Aurelio and Peña, 2010). The inset depicts the location of Palawan relative to Southeast Asia. The structural transect (modified from Aurelio et al., 2014) features emplacement of the thrust-faulted ophiolites over the Eocene Panas Formation which is sealed by the Miocene sequences. (For interpretation of the references to color in this figure legend, the reader is referred to the web version of this article.)

Table 1
Geographic location and stratigraphic context of the samples analyzed in this study.

Sample	Geographic location	Latitude (N)	Longitude (E)	Borehole/Measured depth (m)	Lithology	Previous stratigraphic framework	Youngest zircon U–Pb age (Ma, 1σ uncertainty)	Assigned depositional age
P015	North Palawan	10°31′47.72″	119°19′04.11″		schist	Guinlo Fm.	80 ± 2	Late Cretaceous
P017		10°19′18.13″	119°20′10.00″		metasandstone	Guinlo Fm.	81 ± 2	Late Cretaceous
P018		10°19′18.13″	119°20′10.00″		sandstone	Guinlo Fm.	74 ± 2	Late Cretaceous
P019		10°19′18.13″	119°20′10.00″		metasandstone	Guinlo Fm.	84 ± 2	Late Cretaceous
P022		10°50′11.10″	119°20′58.48″		sandstone	Guinlo Fm.	89 ± 2	Late Cretaceous
P023		10°50′11.10″	119°20′58.48″		sandstone	Guinlo Fm.	96 ± 2	Late Cretaceous
P010		10°05′57.15″	119°12′42.98″		schist	Boayan Fm.	67 ± 2	Late Cretaceous
P011		10°11′56.30″	118°54′09.41″		sandstone	Boayan Fm.	76 ± 4	Late Cretaceous
P026	South Palawan	8°42′27.68″	117°20′23.84″		sandstone	Panas Fm.	62 ± 2	Eocene
P027		8°42′27.68″	117°20′23.84″		sandstone	Panas Fm.	91 ± 3	Eocene
P028		8°44′23.72″	117°23′52.70″		sandstone	Panas Fm.	84 ± 3	Eocene
P029		8°44′22.84″	117°23′48.35″		sandstone	Panas Fm.	87 ± 2	Eocene
P031		9°28′02.65″	118°27′58.36″		sandstone	Panas Fm.	65 ± 1	Eocene
P032		9°01′28.56″	118°03′38.98″		sandstone	Panas Fm.	64 ± 2	Eocene
S1-1	Tainan Basin			S1/3856	sandstone	Lower Cretaceous	127 ± 3	Early Cretaceous
C9-1				C9/3627	sandstone	Upper Cretaceous	128 ± 4	Late Cretaceous
C10-1				C10/3691	sandstone	Upper Cretaceous	134 ± 4	Late Cretaceous
D2-1				D2/2750	sandstone	Eocene	58 ± 2	Eocene
T1-1				T1/907	sandstone	Eocene	104 ± 2	Eocene
L35-2	Pearl River Mouth Basin			L35/2000	sandstone	Upper Jurassic	138 ± 3	Early Cretaceous
L35-1				L35/1300	sandstone	Cretaceous	90 ± 2	Late Cretaceous
B23-2	Qiongdongnan Basin			B23/2326	sandstone	Pre-Cenozoic	107 ± 3	Early Cretaceous
B23-1				B23/2166	sandstone	Pre-Cenozoic	85 ± 3	Late Cretaceous

3. Samples and methods

14 outcrop samples from Palawan and 9 borehole samples from several localities along the northern SCS margin were collected (Fig. 1b). Detailed sample locations and stratigraphic contexts are summarized in Table 1. The stratigraphic ages of borehole samples were based on unpublished seismic and paleontological data from China National Offshore Oil Corporation (CNOOC). The previous stratigraphic framework was further amended by the youngest zircon ages newly acquired in this study, and the stud-

ied samples were assigned to three stratigraphic intervals, i.e., Lower Cretaceous, Upper Cretaceous, and Eocene. Ages of stratigraphic boundaries followed the International Chronostratigraphic Chart v2017/02.

Heavy mineral analysis was conducted on Palawan samples in the laboratory of the Institute of Regional Geology and Mineral Resources, Hebei, China. Samples were heated to dryness and then gently disaggregated using a pestle and mortar. Following disaggregation, the samples were sieved through a 420 μm mesh. Detrital heavy mineral components were separated from bulk sediments by centrifugal elutriation. Further mineral separation was achieved by magnetic and electrostatic filters and heavy liquids. A total of about 1000 non-opaque detrital grains were identified under the binocular microscope.

U–Pb dating was performed by laser ablation-inductively coupled plasma–mass spectroscopy (LA-ICP-MS) and cathodoluminescence images were used to locate analytical spots (20–30 μm) in zircon oscillatory zoning. Zircons from borehole samples were analyzed in the Department of Earth and Environmental Sciences (National Chung Cheng University, Taiwan) in 2014, following the methods described by Knittel et al. (2014). The instrumentation comprises an Agilent 7500a ICP-MS coupled to a New Wave 213 nm LA system. Zircons from Palawan samples were dated in the State Key Laboratory of Marine Geology (Tongji University, China) in 2016, using a Thermo Elemental X-Series ICP-MS coupled to a New Wave 213 nm LA system (Shao et al., 2016).

U–Th–Pb isotopic ratios were calculated using ICPMSDataCal (Liu et al., 2009) followed by the common Pb correction method of Andersen (2002). The accepted ages were selected from a subset of both $\leq$10% discordance and $\leq$10% uncertainty (1σ), wherein the $^{206}Pb/^{238}U$ and $^{207}Pb/^{206}Pb$ ages were adopted for zircons younger and older than 1000 Ma, respectively. If available, this age cutoff criterion was also applied to other published data in this study. Visualization of U–Pb age distributions as histograms and kernel density estimation (KDE) spectra (adaptive bandwidth $\leq$30 Ma) was achieved using the R package named Provenance (Vermeesch et al., 2016).

4. Results

4.1. Heavy minerals

The detrital heavy mineral percentages of 14 Palawan samples are given in Supplementary Table S2 and graphically shown in Fig. 5 along with other published data. In general, the major types of heavy minerals within each formation are basically identical. The Guinlo Formation samples from North Palawan (P015, P017, P018, P019, P022, and P023) have a remarkably high percentage of zircons with an average value of 98.2%. This zircon-dominant mineral assemblage is also seen in the overlying Boayan Formation of the Barton Group (P010 and P011), which is consistent with the heavy mineral results of previous samples PAL-21, PAL-24, PAL-19, PAL-31, and PAL-5 (Suggate et al., 2014). Zircon is still abundant in the Panas Formation of South Palawan (samples P026, P027, P028, P029, P031, and P032), albeit with relatively lower percentages (70.6%–92.7%) compared to the Mesozoic strata of North Palawan. Meanwhile, the Panas Formation samples show a new group of rutile, anatase, and monazite, with minor abundances of tourmaline and spinel. The mineral types in the Eocene Rajang Group and Crocker Fan of North Borneo are largely comparable to those in the Panas Formation, but with appreciably more tourmalines (38.5% and 46.7%) and fewer zircons (36.9% and 27.2%) (van Hattum et al., 2013).

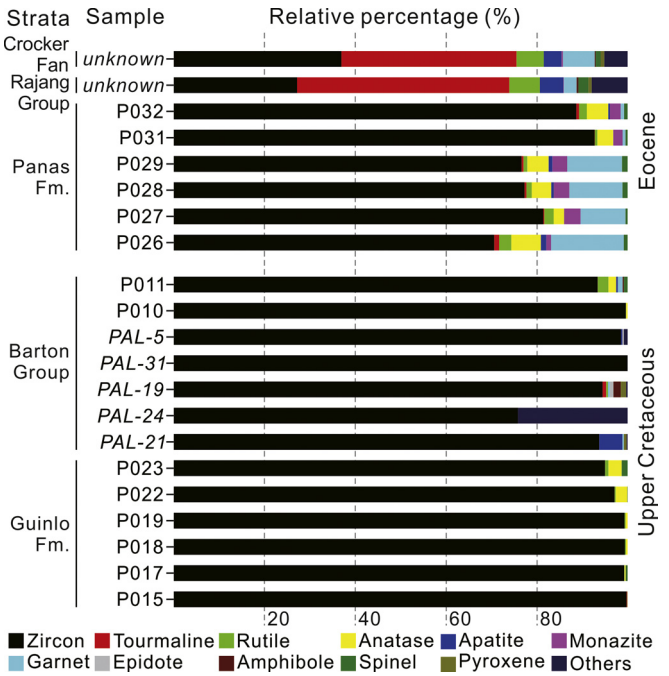

Fig. 5. Heavy mineral assemblages of the Upper Cretaceous and Eocene sediments from Palawan and North Borneo. Published samples (van Hattum et al., 2013; Suggate et al., 2014) are marked with italic font. (For interpretation of the references to color in this figure legend, the reader is referred to the web version of this article.)

4.2. Zircon U–Pb ages

The LA-ICP-MS U–Pb age results of 23 analyzed samples are given in Supplementary Table S3. The youngest single zircon age (Dickinson and Gehrels, 2009) of each sample is summarized in Table 1 to illustrate an improvement in the regional stratigraphic framework. The zircon age ranges of most samples conform to the 'law of detrital zircons': a sedimentary unit can be no older than the youngest zircon grains. However, there are several exceptions to this pattern, which can be best exemplified by the Guinlo Formation samples. Based on stratigraphic position of outcrops, the fossil-poor Guinlo Formation was previously assigned a Late Jurassic–Early Cretaceous age (Fig. 4; Aurelio and Peña, 2010). The youngest single zircon age obtained from samples P015, P017, P018, P019, P022, and P023 ranges from 96 $\pm$ 2 to 74 $\pm$ 2 Ma (Table 1), which constrains the depositional age of the Guinlo Formation to within the Late Cretaceous. This formation is probably a little older than the overlying Boayan Formation where the youngest zircon from samples P010 and P011 was dated at 67 $\pm$ 2 and 76 $\pm$ 4 Ma, respectively (Table 1). Likewise, we assigned a depositional age of Early Cretaceous to samples L35-2 and B23-2, and Late Cretaceous to samples L35-1 and B23-1.

The age data obtained in this study are plotted as histograms and KDEs in Supplementary Fig. S1, and their distribution patterns are described through a comparison with other published data from the SCS region (e.g., West Taiwan and North Borneo; Fig. 1) in order to fully reflect the complexity and diversity of detrital age signatures. However, published U–Pb ages from the pre-Cenozoic basement exposure in Central Taiwan (Tananao Metamorphic Complex) were not compared here because there has been considerable debate regarding its stratigraphy and metamorphism (e.g., Chen et al., 2017). As a complementary approach to the traditional visual examination of age distributions (Fig. 6), a Kolmogorov–Smirnov test-based statistical technique called multidimensional scaling (MDS; Vermeesch et al., 2016) is also employed here to

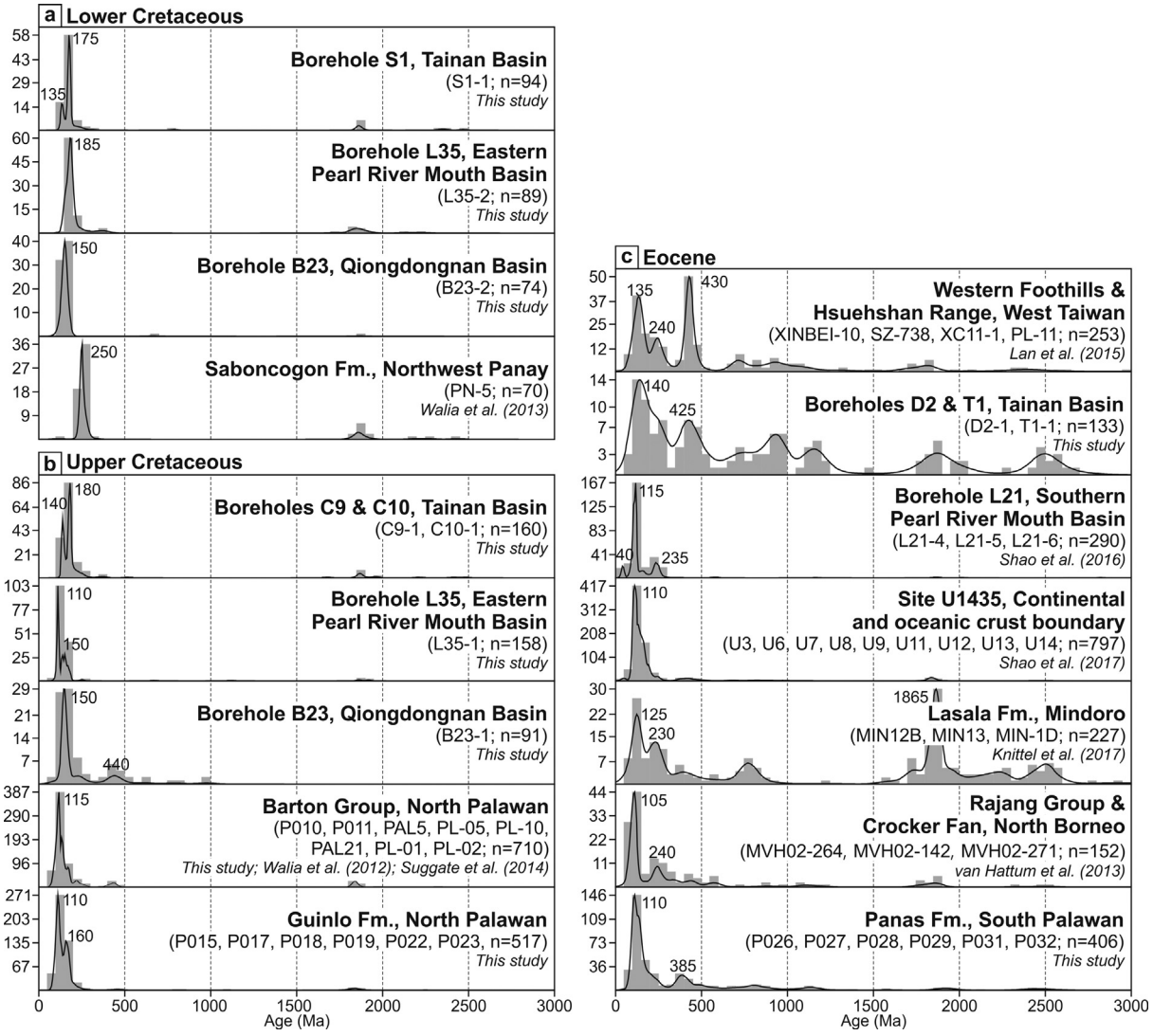

Fig. 6. Detrital zircon U–Pb age signatures of the (a) Lower Cretaceous, (b) Upper Cretaceous, and (c) Eocene samples from the SCS region, shown as histograms and KDE spectra. Sample names and numbers of concordant analyses are shown in parentheses. Published data for the Cretaceous samples include the Saboncogon Formation of Northwest Panay (Walia et al., 2013) and the Barton Group of North Palawan (Walia et al., 2012; Suggate et al., 2014). Published data for the Eocene samples include formations from West Taiwan (Lan et al., 2016), the southern Pearl River Mouth Basin (Shao et al., 2016), the continental-oceanic crust boundary (Shao et al., 2017), Mindoro (Knittel et al., 2017), and North Borneo (van Hattum et al., 2013). See Supplementary Table S4 for compiled samples and age data.

quantitatively assess the relative dissimilarities of multisample age signatures (Fig. 7).

In this study, the Lower Cretaceous record in the northern SCS margin is limited to three boreholes (Fig. 1b). Sample S1-1 from the Tainan Basin and sample L35-2 from the eastern Pearl River Mouth Basin are grouped together at the top of the MDS map (Fig. 7), showing a dominance of Jurassic zircons (Fig. 6a). By contrast, a strong age peak at ca. 150 Ma is seen in sample B23-2 from the Qiongdongnan Basin. In the south, although detrital zircon record of the Lower Cretaceous is missing in Palawan, sample PN-5 from the nearby Saboncogon Formation of Northwest Panay, previously considered as the Jurassic strata equivalent to the Guinlo Formation (Fig. 4; Aurelio and Peña, 2010), contains a single 118-Ma zircon grain as well as abundant Permian–Triassic zircons (Walia et al., 2013).

The age KDEs of zircons from boreholes C9 and C10 as well as the adjacent borehole S1 are compatible, indicating an unchanged age distribution pattern of the Cretaceous Tainan Basin (Figs. 6b and S1). By contrast, a cluster of Paleozoic to Early Mesozoic zircons is newly detected in sample B23-1 from the Qiongdongnan Basin. Meanwhile, zircon ages in the Cretaceous samples from the eastern Pearl River Mouth Basin are characterized by an overall younging trend, with the dominant age peak changing from ca. 185 Ma in L35-2 to ca. 110 Ma in L35-1. In the Upper Cretaceous strata of North Palawan (Guinlo Formation and Barton Group), zircon, as a dominant heavy mineral (Fig. 5), is generally dated with Middle–Late Mesozoic ages (Fig. S1). However, the KDE pattern of each sample shows a certain degree of dissimilarity, as supported by their scattered distribution on the left side of the MDS plot (Fig. 7). Regardless of this intra-formational variation, it is noteworthy for the comparison of compiled data that the age signature of the Guinlo Formation exhibits a high resemblance to that of sample L35-1, but slightly differs from that of the Barton Group with fewer Jurassic ages (Fig. 6b).

In contrast to an apparent dominance of Mesozoic zircons in the Cretaceous strata, older zircons are commonly present in the Eocene strata from different localities of the SCS region (Fig. 6c). However, the MDS results clearly show that the age signatures vary to a great degree among these Eocene samples (Fig. 7). More specifically, samples from the Western Foothills and Hsuehshan Range of West Taiwan (XINBEI-10, SZ-738, XC11-1, and PL-11) display three major age peaks at ca. 135 Ma, ca. 240 Ma, and

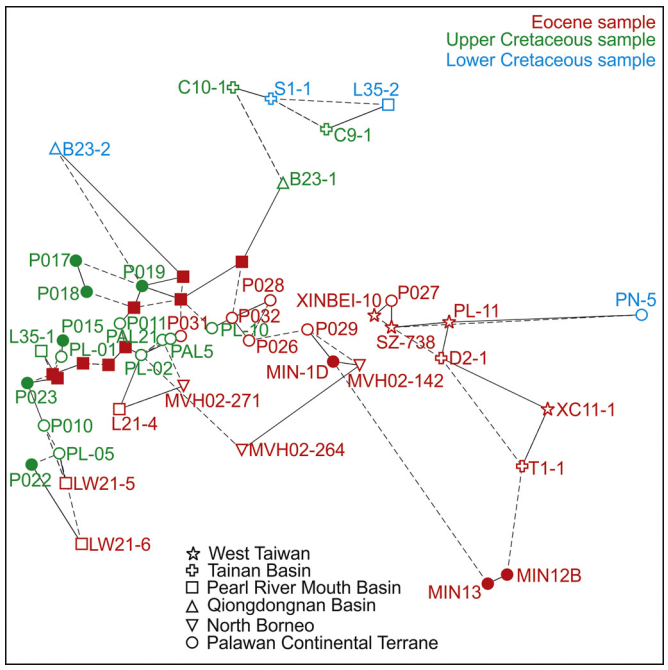

Fig. 7. Nonmetric multidimensional scaling (MDS; Vermeesch et al., 2016) map for compiled detrital zircon U–Pb ages of the Cretaceous and Eocene samples. The stress value of MDS statistics is 0.097, indicating a fair goodness-of-fit. This plot groups the samples with similar age spectra, with solid and dashed lines marking the closest and the second closest neighbors, respectively. The filled red squares without names represent U1435 samples. The PCT samples of the Upper Cretaceous include those from the Guinlo Formation (filled green circles) and the Barton Group (open green circles) of North Palawan. The PCT samples of the Eocene include those from the Panas Formation of South Palawan (open red circles) and the Lasala Formation of Mindoro (filled red circles). All age data follow those given in Fig. 6. (For interpretation of the references to color in this figure legend, the reader is referred to the web version of this article.)

ca. 430 Ma as well as a minor population of Proterozoic ages (Lan et al., 2016). The KDEs of samples D2-1 and T1-1 from the Tainan Basin, albeit somewhat smoothed, are comparable to those of the Taiwan samples (Figs. 6c and S1), as also recognized by their close linkages in the MDS plot (Fig. 7). By contrast, coeval samples to the west from both commercial borehole L21 (L21-4, L21-5, and L21-6) and International Ocean Discovery Program (IODP) Site U1435 (U3, U6, U7, U8, U9, U11, U12, U13, and U14) are dominated by Cretaceous zircons with a scarcity of Proterozoic to Paleozoic zircons (Figs. 1b and 6c; Shao et al., 2016, 2017). The former KDE slightly differs from the latter in showing two minor peaks at ca. 40 Ma and ca. 235 Ma. In the southern SCS margin, the large U–Pb age range and multimodal spectra also characterize samples from the deep marine Lasala Formation of Mindoro (Fig. 6c; Knittel et al., 2017). The extremely high percentage of Paleoproterozoic zircons, however, makes two of these samples (MIN12B and MIN13) separate from other groups in the MDS plot (Fig. 7). Farther south, zircons from the Rajang Group and Crocker Fan of North Borneo (samples MVH02-264, MVH02-142, and MVH02-271) are mostly dated with Cretaceous and Triassic ages peaking at ca. 105 Ma and ca. 240 Ma, respectively (van Hattum et al., 2013). In this study, six samples from the Panas Formation of South Palawan (P026, P027, P028, P029, P031, and P032) are plotted together at the center of the MDS map (Fig. 7), showing consistent KDE characteristics with a prominent Early Cretaceous peak at ca. 110 Ma as well as a certain percentage (28.0%–52.7%) of Proterozoic to Paleozoic populations (Figs. 6c and S1).

5. Provenance and paleogeographic reconstruction

5.1. Early Cretaceous

During the Early Cretaceous, the northern SCS region was generally dominated by a littoral to lacustrine environment (Shao et al., 2007; Li et al., 2008). An absence of Mesoproterozoic–Early Mesozoic age peaks in samples from the relic basins there, when compared against the age signatures of modern source areas (Figs. 3 and 6a), precludes the possibility of long-distance sediment transport from the hinterland of Indochina and South China. By contrast, the abundant Jurassic zircons were likely derived from magmatic arcs along the South China margin, while a smaller number of zircons with dates between 1900 and 1800 Ma could have been recycled from the oldest crystalline basement of Cathaysia (Zhou and Li, 2000; Li et al., 2012). In addition, 43% of zircons from the Qiongdongnan Basin (sample B23-2) and 18% from the Tainan Basin (sample S1-1) are younger than 145 Ma, suggesting an input from syn-depositional magmatism. Although the Lower Cretaceous record of Palawan was unfortunately not available for this study, the unique zircon age population peaking at ca. 250 Ma in sample PN-5 from the easternmost PCT (Fig. 6a) has been interpreted to be sourced from the nearby Halcon Metamorphics of Mindoro where a metagranodiorite yielded a quite similar emplacement age (Walia et al., 2013). Meanwhile, the Halcon Metamorphics could be possibly correlated with the contemporary igneous rocks in coastal South China and Indochina (Figs. 1 and 3), representing low-volume syn-orogenic magmatism outboard the East Asian margin during the Hercynian–Indosinian orogeny (Holloway, 1982; Li et al., 2012).

5.2. Late Cretaceous

A large body of evidence from paleoaltimetric, stratigraphic, and paleoclimatic studies suggests that there were still extensive coastal mountains along the continental China margin during the Late Cretaceous (e.g., Wang, 2004; Li et al., 2014; Zhang et al., 2016). Based on the restricted zircon age distribution patterns (Fig. 6b), potential sources from continental arcs continued to contribute considerably to the Upper Cretaceous infill of the northern SCS region (Fig. 8a). However, the spatial distribution of the Late Mesozoic subduction zone was clearly non-stationary, which can be best exemplified by the oceanward younging trend of the Yanshanian magmatism in this continental arc system (Zhou and Li, 2000; Li et al., 2014). It may be possible to recognize the corresponding compositional variations in relic basins along the South China margin. Here it is noteworthy that, from Early to Late Cretaceous, the eastern Pearl River Mouth Basin was characterized by a younging trend of major zircon age peaks, whereas a larger range of zircon ages occurred in the Qiongdongnan Basin (Figs. 6a and 6b), possibly pointing to a retreat of long segments of continental arcs towards the southeast. Alternatively, these age signature variations could be caused by provenances from local bedrocks because sediment transport paths would tend to change during the Cretaceous marine regression (Shao et al., 2007; Sun et al., 2014).

A ca. 83-Ma rhyolite locally exposed in North Mindoro provides a correlation of contemporaneous felsic magmatism between the South China margin and the PCT (Knittel et al., 2017). The remarkable similarity of age signatures between the Guinlo Formation of North Palawan and sample L35-1 from the eastern Pearl River Mouth Basin (Figs. 6b and 7) indicates a likely common source area for these contemporary sediments although they now lie thousands of miles apart (Fig. 8a). Although 500–400-Ma zircons are found in the Barton Group (Fig. 6b), their relative percentage (less than 5%) appears too low to account for a direct source-to-sink

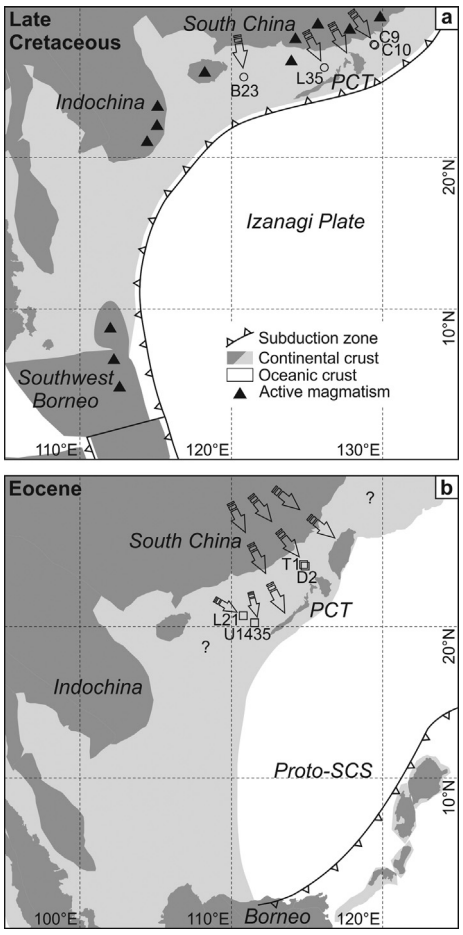

Fig. 8. Paleogeographic reconstruction of the PCT (modified from Hall, 2002; Breitfeld et al., 2017), showing provenance evolution in the northern SCS region from (a) Late Cretaceous to (b) Eocene. The localities of studied boreholes are schematically marked. Arrows stand for interpreted sediment dispersal routes from source areas to the studied sites. In the Late Cretaceous, the studied sites were in a forearc region with major sediment supply from nearby continental arcs, and North Palawan of the PCT could be located close to the present-day eastern Pearl River Mouth Basin where borehole L35 was drilled. In the Eocene, the PCT was probably flanked by rift basins of the South China margin in the north and the Proto-SCS in the south. Note the distinct sediment dispersal routes in the northeastern SCS region and the outer Pearl River Mouth Basin, with their potential provenances originating from distal southeastern South China and local intrabasinal uplifts, respectively.

relationship between the Caledonian orogenic belt in South China and Palawan. A zircon-dominant heavy mineral assemblage (Fig. 5), abundant felsic volcanic rock fragments (Suzuki et al., 2000), and up to 11% zircons produced by syn-depositional magmatism together also support a forearc position for the Late Cretaceous PCT (Fig. 8a).

5.3. Eocene

The termination of the Mesozoic continental arc system was recently suggested at ca. 70 Ma based on the youngest emplacement ages of subduction-related granitoids found in the Pearl River Mouth Basin (Yan et al., 2014). The prolonged extension from Late Cretaceous to Early Cenozoic resulted in the collapse of preexisting coastal mountains and the formation of half-grabens and grabens in the rift zone (Lin et al., 2003; Morley, 2016). Meanwhile, due to diachronous rifting, marine deposition was dominant during the Eocene in the northeast of the SCS region, whereas continental to transitional deposition dominated in the southwest (Li et al., 2016). These variations in both topography and depositional environment could substantially influence the sediment transport process and perhaps the sediment composition in the northern SCS margin.

Compared to the multimodal zircon age distributions of modern drainage sediments from South China (Figs. 1 and 3), the very restricted age range of zircons from both borehole L21 and Site U1435 (Fig. 6c) clearly indicates that local inputs from preexisting Mesozoic rocks of intrabasinal uplifts could have contributed more than other distant sources to the Eocene infill of the outer Pearl River Mouth Basin (Fig. 8b; Shao et al., 2016, 2017). However, determining the exact locations of these local provenances cannot be easily achieved due to limited borehole coverage. By contrast, there existed a possible source-to-sink relationship between southeastern South China and the northeastern SCS region (Fig. 8b), based on the large zircon age range and multimodal KDEs of the Eocene marine strata from the Tainan Basin and Taiwan (Fig. 6c). Potential provenances from western South China and Indochina appear not to be significant because of the lack of Late Mesozoic zircons in parent rocks (Figs. 1 and 3).

The very high percentage (average value = 81.2%) of detrital zircons (Fig. 5), with a large range of U–Pb crystallization ages (Fig. 6c), newly acquired from the Panas Formation of Palawan confirm a continental affinity similar to the contemporary Lasala Formation of Mindoro (Knittel et al., 2017). By contrast, the mafic nature of ophiolitic provenance did not become characteristic until the Miocene, as manifested by the heavy mineral assemblage of epidote–amphibole–spinel–pyroxene in the overlying Isugod Formation sandstones from South Palawan (Fig. 4; Suggate et al., 2014). Thus, the provenance interpretation of the Cenozoic sequences from South Palawan indicates that, despite the present-day surface exposure of ophiolites, South Palawan still tectonically constitutes a part of the PCT, which is consistent with the recent stratigraphic study by Aurelio et al. (2014).

If the southward drift of the PCT was caused by the latest Cretaceous backarc spreading of the Proto-SCS (Fig. 2c; Morley, 2012; Zahirovic et al., 2014), the PCT would have been in an intra-oceanic position since that time and its Eocene sediment composition would likely inherit the arc-derived nature of Mesozoic parent rocks. However, this is not supported by our data with a clear Late Cretaceous–Eocene provenance shift that a larger range of zircon ages as well as a new heavy mineral group (rutile, anatase, and monazite) are identified in the Panas Formation (Figs. 5 and 6c). Although a spread of Proterozoic to Paleozoic zircons existed in the Eocene marine sediments from both Palawan and North Borneo (Fig. 6c), their possible stratigraphic linkage is ruled out based on their distinct heavy mineral assemblages (Fig. 5). Moreover, the dominant Cretaceous zircons in Borneo samples have been interpreted to be sourced from the nearby granitic Schwaner Mountains as indicated by the strikingly immature texture and poor sorting of bulk sandstones (van Hattum et al., 2013). Thus, separation of the PCT from the South China margin prior to the Oligocene SCS oceanization is unlikely, and the Palawan Trough is not an ancient trench formed by the Proto-SCS subduction as previously hypothesized (Fig. 2c; Hutchison, 2010; Cullen, 2014). Although the origin and extent of the Proto-SCS cannot be determined from our provenance data, during the Eocene the PCT could probably exist as a passive margin to the north of the Proto-SCS oceanic crust (Fig. 8b; Taylor and Hayes, 1983; Hall, 2002; Keenan et al., 2016).

Although the extensional setting in the SCS region could start as early as the Late Cretaceous, the rifting process was episodic in nature and most of the margin surface area newly formed during rift extension was likely created in a short period of time before crustal breakup of the SCS (Brune et al., 2016). The large age range of zircons in both South Palawan and Mindoro (Fig. 6c) may suggest that the PCT remained attached to the northern margin in the Eocene, and received sediment supply from common sources

alongside with the Tainan Basin and Taiwan (Fig. 8b). This provenance interpretation is largely consistent with not only the proposed Late Cretaceous location of the PCT in proximity to the eastern Pearl River Mouth Basin (Fig. 8a), but also the widespread marine environment in the northeastern SCS region during the Eocene (Li et al., 2016). In this case, the compositional change along the South China margin from Late Cretaceous to Eocene tends to mark a large-scale tectonic-driven provenance shift corresponding to the transition from an active margin setting of South China during the Panthalassa subduction to a passive margin setting related to diachronous and episodic continental rifting preceding the SCS opening (Fig. 8). The percentage differences in major zircon populations of the Eocene strata among Taiwan, Taixinan Basin, South Palawan, and Mindoro can be probably explained by various factors including topographic, lithological, and environmental configurations. However, distinguishing their specific source terranes requires a detailed comparison with more compositional data from modern drainage basins as well as a larger sample coverage in the East China Sea and the northern Pearl River Mouth Basin, which would be beyond the scope of this study. Nevertheless, the significant provenance supply from distal southeastern South China to the SCS region would likely continue until the west-tilting topography of East Asia was reversed with major fluvial systems derived from the uplifted Tibetan Plateau (Wang, 2004).

6. Conclusions

By comparing the heavy mineral and detrital zircon U–Pb age signatures of Cretaceous and Eocene strata from the PCT and the northern SCS margin, this study provides a provenance perspective on regional paleogeographic reconstruction that enables us to determine where and when the PCT was separated from its conjugate margin. Our results reveal a significant Cretaceous–Eocene provenance shift along the South China margin, which is interpreted to be caused by the regional tectonic transition from an active margin setting in the Mesozoic to a passive margin setting in the Early Cenozoic. The provenance for the Cretaceous strata of the northeastern SCS region was mainly derived from nearby continental arcs, featuring a rather limited range of zircon ages with Yanshanian peaks, whereas the multimodal distribution and large range of zircon ages of the Eocene strata are compatible with the age signatures of modern drainage sediments from southeastern South China. A similar trend in zircon age distributions is also observed in the contemporary strata of the PCT. Meanwhile, the heavy mineral data from Palawan show a change from the zircon-dominant mineral assemblage in the Cretaceous strata to the newly detected group of rutile, anatase, and monazite in the Eocene strata. Both lines of evidence suggest that a latest Cretaceous drift of the PCT caused by the Proto-SCS opening is unlikely, because in this model, the PCT would be in an intra-oceanic position during the Eocene with sediment provenance probably from the arc-derived Mesozoic parent rocks. Instead, the PCT was attached to the South China margin from the Cretaceous until the Oligocene oceanization of the SCS, mostly likely as a conjugate to the eastern Pearl River Mouth Basin based on their comparable provenance signatures.

Admittedly, the evolution of the entire source-to-sink system over such time scales could be more complex than we present here, which can be exemplified by the local provenance signatures in the Late Cretaceous Qiongdongnan Basin and the Eocene outer Pearl River Mouth Basin. Future research should extend the sample coverage in terms of both geography (e.g., Macclesfield Bank and Reed Bank) and stratigraphy (e.g., Lower Cretaceous and Paleocene) in order to increase sample representativeness of particular source terranes and to verify the provenance interpretations proposed in this study. Meanwhile, detrital zircon U–Pb geochronology has been shown to be a powerful tool in constraining the depositional age of fossil-poor strata like the Guinlo Formation of North Palawan, and can continue to be employed to help establish a more reliable regional stratigraphic framework.

Acknowledgements

We thank China National Offshore Oil Corporation (CNOOC) for providing geological data and borehole samples from the northern South China Sea. Alyssa Peleo-Alampay and Allan Gil S. Fernando kindly introduced us the geology of Palawan during a field trip together with Chi-Yue Huang, Xixi Zhao, and Changhai Xu. We also thank Christopher K. Morley for commenting on an earlier version of this paper. Constructive reviews by two anonymous referees and editorial handling by An Yin are gratefully appreciated. This work was supported by the National Natural Science Foundation of China (grant numbers 91128207, 41576059, and 91228203) and the National Science and Technology Major Project (grant number 2011ZX05023-03). DJJvH acknowledges ERC Starting grant 306810 (SINK) and NWO VIDI grant 864.11.004. LC acknowledges the China Scholarship Council for supporting his study at Utrecht University.

Appendix A. Supplementary material

Supplementary material related to this article can be found online at http://dx.doi.org/10.1016/j.epsl.2017.08.019.

References

Almasco, J.N., Rodolfo, K., Fuller, M., Frost, G., 2000. Paleomagnetism of Palawan, Philippines. J. Asian Earth Sci. 18, 369–389.
Andersen, T., 2002. Correction of common lead in U–Pb analyses that do not report ^{204}Pb. Chem. Geol. 192, 59–79.
Aurelio, M.A., Forbes, M.T., Taguibao, K.J.L., Savella, R.B., Bacud, J.A., Franke, D., Pubellier, M., Savva, D., Meresse, F., Steuer, S., Carranza, C.D., 2014. Middle to Late Cenozoic tectonic events in south and central Palawan (Philippines) and their implications to the evolution of the south-eastern margin of South China Sea: evidence from onshore structural and offshore seismic data. Mar. Pet. Geol. 58 (B), 658–673.
Aurelio, M., Peña, R., 2010. Stratigraphy and petrology (Palawan Island). In: Aurelio, M., Peña, R. (Eds.), Geology of the Philippines, second edition. Mines and Geosciences Bureau, Quezon City, pp. 236–265.
Bai, Y., Wu, S., Liu, Z., Müller, R.D., Williams, S.E., Zahirovic, S., Dong, D., 2015. Full-fit reconstruction of the South China Sea conjugate margins. Tectonophysics 661, 121–135.
Breitfeld, H.T., Hall, R., Galin, T., Forster, M.A., BouDagher-Fadel, M.K., 2017. A Triassic to Cretaceous Sundaland–Pacific subduction margin in West Sarawak, Borneo. Tectonophysics 694, 35–56.
Briais, A., Patriat, P., Tapponnier, P., 1993. Updated interpretation of magnetic anomalies and seafloor spreading stages in the south China Sea: implications for the Tertiary tectonics of Southeast Asia. J. Geophys. Res. 98, 6299–6328.
Brune, S., Williams, S.E., Butterworth, N.P., Müller, R.D., 2016. Abrupt plate accelerations shape rifted continental margins. Nature 536, 201–204.
Chen, W.-S., Chung, S.-L., Chou, H.-Y., Zul, Z., Shao, W.-Y., Lee, Y.-H., 2017. A reinterpretation of the metamorphic Yuli belt: evidence for a middle–late Miocene accretionary prism in eastern Taiwan. Tectonics 36, 188–206.
Cullen, A., 2014. Nature and significance of the West Baram and Tinjar Lines, NW Borneo. Mar. Pet. Geol. 51, 197–209.
Dickinson, W.R., Gehrels, G.E., 2009. Use of U–Pb ages of detrital zircons to infer maximum depositional ages of strata: a test against a Colorado Plateau Mesozoic database. Earth Planet. Sci. Lett. 288, 115–125.
Encarnación, J.P., Essene, E.J., Mukasa, S.B., Hall, C.H., 1995. High-pressure and -temperature subophiolitic kyanite—garnet amphibolites generated during initiation of mid-Tertiary subduction, Palawan, Philippines. J. Petrol. 36, 1481–1503.
Franke, D., Savva, D., Pubellier, M., Steuer, S., Mouly, B., Auxietre, J.-L., Meresse, F., Chamot-Rooke, N., 2014. The final rifting evolution in the South China Sea. Mar. Pet. Geol. 58 (B), 704–720.
Hall, R., 2002. Cenozoic geological and plate tectonic evolution of SE Asia and the SW Pacific: computer-based reconstructions, model and animations. J. Asian Earth Sci. 20, 353–431.
Holloway, N.H., 1982. North Palawan Block, Philippines—its relation to Asian Mainland and role in evolution of South China Sea. AAPG Bull. 66, 1355–1383.
Hutchison, C.S., 2010. The North-West Borneo Trough. Mar. Geol. 271, 32–43.
Keenan, T.E., Encarnacion, J., Buchwaldt, R., Fernandez, D., Mattinson, J., Rasoazanamparany, C., Luetkemeyer, P.B., 2016. Rapid conversion of an oceanic

spreading center to a subduction zone inferred from high-precision geochronology. Proc. Natl. Acad. Sci. USA 113, E7359–E7366.
Knittel, U., Suzuki, S., Nishizaka, N., Kimura, K., Tsai, W.-L., Lu, H.-Y., Ishikawa, Y., Ohno, Y., Yanagida, M., Lee, Y.-H., 2014. U–Pb ages of detrital zircons from the Sanbagawa Belt in western Shikoku: additional evidence for the prevalence of Late Cretaceous protoliths of the Sanbagawa Metamorphics. J. Asian Earth Sci. 96, 148–161.
Knittel, U., Walia, M., Suzuki, S., Dimalanta, C.B., Tamayo, R., Yang, T.F., Yumul, G.P., 2017. Diverse protolith ages for the Mindoro and Romblon Metamorphics (Philippines): evidence from single zircon U–Pb dating. Isl. Arc 26, 1–17.
Lan, Q., Yan, Y., Huang, C.-Y., Santosh, M., Shan, Y.-H., Chen, W., Yu, M., Qian, K., 2016. Topographic architecture and drainage reorganization in Southeast China: zircon U–Pb chronology and Hf isotope evidence from Taiwan. Gondwana Res. 36, 376–389.
Leloup, P.H., Arnaud, N., Lacassin, R., Kienast, J.R., Harrison, T.M., Trong, T.T., Replumaz, A., Tapponnier, P., 2001. New constraints on the structure, thermochronology, and timing of the Ailao Shan–Red River shear zone, SE Asia. J. Geophys. Res., Solid Earth 106, 6683–6732.
Li, Z.-X., Li, X.-H., Chung, S.-L., Lo, C.-H., Xu, X., Li, W.-X., 2012. Magmatic switch-on and switch-off along the South China continental margin since the Permian: transition from an Andean-type to a Western Pacific-type plate boundary. Tectonophysics 532–535, 271–290.
Li, Q., Wu, G., Zhang, L., Shu, Y., Shao, L., 2016. Paleogene marine deposition records of rifting and breakup of the South China Sea: an overview. Sci. China Earth Sci., 1–13.
Li, J., Zhang, Y., Dong, S., Johnston, S.T., 2014. Cretaceous tectonic evolution of South China: a preliminary synthesis. Earth-Sci. Rev. 134, 98–136.
Li, C.-F., Zhou, Z., Hao, H., Chen, H., Wang, J., Chen, B., Wu, J., 2008. Late Mesozoic tectonic structure and evolution along the present-day northeastern South China Sea continental margin. J. Asian Earth Sci. 31, 546–561.
Lin, A.T., Watts, A.B., Hesselbo, S.P., 2003. Cenozoic stratigraphy and subsidence history of the South China Sea margin in the Taiwan region. Basin Res. 15, 453–478.
Liu, Y., Gao, S., Hu, Z., Gao, C., Zong, K., Wang, D., 2009. Continental and oceanic crust recycling-induced melt-peridotite interactions in the Trans-North China Orogen: U–Pb dating, Hf isotopes and trace elements in zircons from mantle xenoliths. J. Petrol. 51, 537–571.
Morley, C.K., 2012. Late Cretaceous–Early Palaeogene tectonic development of SE Asia. Earth-Sci. Rev. 115, 37–75.
Morley, C.K., 2016. Major unconformities/termination of extension events and associated surfaces in the South China Seas: review and implications for tectonic development. J. Asian Earth Sci. 120, 62–86.
Müller, R.D., Seton, M., Zahirovic, S., Williams, S.E., Matthews, K.J., Wright, N.M., Shephard, G.E., Maloney, K., Barnett-Moore, N., Hosseinpour, M., Bower, D.J., Cannon, J., 2016. Ocean basin evolution and global-scale plate reorganization events since Pangea breakup. Annu. Rev. Earth Planet. Sci. 44, 107–138.
Nagy, E.A., Maluski, H., Thi, P.T., Lepvrier, C., Leyreloup, A., Schärer, U., Thich, a.V.V., 2001. Geodynamic significance of the Kontum Massif in Central Vietnam: composite $^{40}Ar/^{39}Ar$ and U–Pb Ages from Paleozoic to Triassic. J. Geol. 109, 755–770.
Schlüter, H.U., Hinz, K., Block, M., 1996. Tectono-stratigraphic terranes and detachment faulting of the South China Sea and Sulu Sea. Mar. Geol. 130, 39–78.
Shao, L., Cao, L., Pang, X., Jiang, T., Qiao, P., Zhao, M., 2016. Detrital zircon provenance of the Paleogene syn-rift sediments in the northern South China Sea. Geochem. Geophys. Geosyst. 17, 255–269.
Shao, L., Meng, A., Li, Q., Qiao, P., Cui, Y., Cao, L., Chen, S., 2017. Detrital zircon ages and elemental characteristics of the Eocene sequence in IODP Hole U1435A: implications for rifting and environmental changes before the opening of the South China Sea. Mar. Geol. http://dx.doi.org/10.1016/j.margeo.2017.08.002 (in press).
Shao, L., You, H., Hao, H., Wu, G., Qiao, P., Lei, Y., 2007. Petrology and depositional environments of Mesozoic Strata in the Northeastern South China Sea. Geol. Rev. 53, 164–169 (in Chinese with English abstract).
Sibuet, J.-C., Yeh, Y.-C., Lee, C.-S., 2016. Geodynamics of the South China Sea. Tectonophysics 692 (B), 98–119.
Suggate, S.M., Cottam, M.A., Hall, R., Sevastjanova, I., Forster, M.A., White, L.T., Armstrong, R.A., Carter, A., Mojares, E., 2014. South China continental margin signature for sandstones and granites from Palawan, Philippines. Gondwana Res. 26, 699–718.
Sun, X., Zhang, X., Zhang, G., Lu, B., Yue, J., Zhang, B., 2014. Texture and tectonic attribute of Cenozoic basin basement in the northern South China Sea. Sci. China Earth Sci. 57, 1199–1211.
Suzuki, S., Takemura, S., Yumul, G.P., David, S.D., Asiedu, D.K., 2000. Composition and provenance of the Upper Cretaceous to Eocene sandstones in Central Palawan, Philippines: constraints on the tectonic development of Palawan. Isl. Arc 9, 611–626.
Taylor, B., Hayes, D.E., 1983. Origin and history of the South China Sea basin. In: Hayes, D.E. (Ed.), The Tectonic and Geologic Evolution of Southeast Asian Seas and Islands: Part 2. American Geophysical Union, Washington, DC, pp. 23–56.
van Hattum, M.W.A., Hall, R., Pickard, A.L., Nichols, G.J., 2013. Provenance and geochronology of Cenozoic sandstones of northern Borneo. J. Asian Earth Sci. 76, 266–282.
Vermeesch, P., Resentini, A., Garzanti, E., 2016. An R package for statistical provenance analysis. Sediment. Geol. 336, 14–25.
Walia, M., Knittel, U., Suzuki, S., Chung, S.-L., Pena, R.E., Yang, T.F., 2012. No Paleozoic metamorphics in Palawan (the Philippines)? Evidence from single grain U–Pb dating of detrital zircons. J. Asian Earth Sci. 52, 134–145.
Walia, M., Yang, T.F., Knittel, U., Liu, T.K., Lo, C.H., Chung, S.L., Teng, L.S., Dimalanta, C.B., Yumul, G.P., Yuan, W.M., 2013. Cenozoic tectonics in the Buruanga Peninsula, Panay Island, Central Philippines, as constrained by U–Pb, $^{40}Ar/^{39}Ar$ and fission track thermochronometers. Tectonophysics 582, 205–220.
Wang, P., 2004. Cenozoic deformation and the history of sea–land interactions in Asia. In: Clift, P., Kuhnt, W., Wang, P., Hayes, D. (Eds.), Continent–Ocean Interactions Within East Asian Marginal Seas. American Geophysical Union, Washington, DC, pp. 1–22.
Yan, Q., Shi, X., Castillo, P.R., 2014. The late Mesozoic–Cenozoic tectonic evolution of the South China Sea: a petrologic perspective. J. Asian Earth Sci. 85, 178–201.
Zahirovic, S., Seton, M., Müller, R.D., 2014. The Cretaceous and Cenozoic tectonic evolution of Southeast Asia. Solid Earth 5, 227–273.
Zhang, L., Wang, C., Cao, K., Wang, Q., Tan, J., Gao, Y., 2016. High elevation of Jiaolai Basin during the Late Cretaceous: implication for the coastal mountains along the East Asian margin. Earth Planet. Sci. Lett. 456, 112–123.
Zhou, X.M., Li, W.X., 2000. Origin of Late Mesozoic igneous rocks in Southeastern China: implications for lithosphere subduction and underplating of mafic magmas. Tectonophysics 326, 69–287.